Journal of Hydrology 452–453 (2012) 139–149

Contents lists available at SciVerse ScienceDirect

Journal of Hydrology

journal homepage: www.elsevier.com/locate/jhydrol

Comparison of floodplain surface roughness parameters derived from land cover data and field measurements

Stephen C. Medeiros [a,*], Scott C. Hagen [a,1], John F. Weishampel [b,2]

[a] University of Central Florida, Dept. of Civil, Environmental and Construction Engineering, 4000 Central Florida Blvd., Orlando, FL 32816, USA
[b] University of Central Florida, Dept. of Biology, 4000 Central Florida Blvd., Orlando, FL 32816, USA

ARTICLE INFO

Article history:
Received 24 October 2011
Received in revised form 13 April 2012
Accepted 19 May 2012
Available online 4 June 2012
This manuscript was handled by Konstantine P. Georgakakos, Editor-in-Chief, with the assistance of Ehab A. Meselhe, Associate Editor

Keywords:
Surface roughness
Field measurements
Manning's *n*
Canopy
Effective roughness length

SUMMARY

Parameterizing surface roughness is a key element in the application of tidal and storm surge inundation models. In this context, surface roughness refers to the ability of the terrain to act as a momentum sink to the overland water flow and also the prevailing winds that help drive this flow. These effects are typically parameterized using estimates of Manning's *n*, surface canopy coverage and effective aerodynamic roughness length which vary spatially across the modeling domain as a function of the physical landscape. The current methodology for coastal inundation in the United States assigns these parameters based on published land use/land cover data such as the National Land Cover Dataset. This paper compares those assigned values to values computed based on field measurements at 24 sites in Florida that are representative of land use/land cover classes affected by storm surge. It is shown that while the land use/land cover method is capable of automatically parameterizing surface roughness over a large model domain, parameter prediction errors due to variability within land cover types, misclassification, and parameter value selection for specific land cover classes at the local level are significant which could result in inaccurate estimates of inundation extent and duration.

1. Introduction

The propagation of overland inundation is heavily influenced by the roughness of the terrain surface. It is the most important parameter, after topography, that influences overland flow patterns (Straatsma, 2009). Drag forces exerted on the flow by above-ground obstructions in the floodplain such as trees, grasses, bushes and structures serve to dissipate hydraulic energy and the momentum of the flood wave. These obstructions also modify wind characteristics, an important forcing mechanism in hurricane storm surge modeling. In finite element schemes, these phenomena are parameterized and implemented in the form of bottom friction coefficients (Strelkoff et al., 2009) such as Manning's *n*, along with coefficients that represent the surface canopy closure and effective roughness length (aerodynamic roughness). This study focuses on the parameterization of surface roughness in 2-dimensional, depth integrated models where according to Morvan et al. (2008) "roughness is a model of the physical processes that are omitted" (p. 191) from the governing equations. Two prominent examples of this type of model are TELEMAC-2D (Galland et al., 1991; Hervouet, 2000) and ADCIRC (Luettich and Westerink, 2006; Luettich et al., 1992).

Many studies consider bottom friction to be a calibrated model parameter (Mailapalli et al., 2008); however, more and more researchers are constructing models that seek to describe the physics of the processes as purely as possible, with no calibrated or tuned friction parameters (Atkinson et al., 2011; Bacopoulos et al., 2009; Cobby et al., 2003; Mason et al., 2003; Westerink et al., 2008). Please note that in this context, the terms "calibrated" or "tuned" refer to those models where bottom friction is adjusted using automated optimization algorithms in an effort to improve model results with respect to observed data. All modeling requires some level of engineering judgment and the manual adjustment of bottom friction parameters, within generally accepted ranges, is herein not considered "calibration". Fortunately, many studies have been conducted to assist the modeler in selecting and adjusting bottom friction parameters based on the conditions of the domain.

Past investigations into the determination of the bottom friction coefficient at actual sites throughout the world typically follow one of two methods:

1. Measure flow velocity and topographic conditions (depth and cross-sectional area); or

* Corresponding author. Tel.: +1 407 823 4843; fax: +1 407 823 3315.
E-mail addresses: scm@knights.ucf.edu (S.C. Medeiros), Scott.Hagen@ucf.edu (S.C. Hagen), John.Weishampel@ucf.edu (J.F. Weishampel).
[1] Tel.: +1 407 823 3903; fax: +1 407 823 3315.
[2] Tel.: +1 407 823 6634; fax: +1 407 823 5769.

0022-1694/$ - see front matter © 2012 Elsevier B.V. All rights reserved.
http://dx.doi.org/10.1016/j.jhydrol.2012.05.043

2. Measure topographic conditions and physical characteristics (heights, widths, etc.) of obstacles that impede flow.

Both methodologies then rely on established equations, usually empirical (Burguete et al., 2007), to compute bottom friction.

Following the first method, research has been conducted by Harun-ur-Rashid (1990), Bakry et al. (1992), Vieux and Farajalla (1994), Myers et al. (1999), Sepaskhah and Bondar (2002), Stephan and Gutknecht (2002), Mailapalli et al. (2008), Aricó et al. (2009), among others. Studies of this type employ numerical models that use the topographic data as input and measured flows as initial and boundary conditions. The value for the roughness coefficient is then calibrated to match recorded water levels. Xu and Wright (1995) took this methodology from the rivers and floodplains into the nearshore regions of the Middle Atlantic Bight and tested roughness models with emphasis on grain, ripple and sediment motion roughness. Li and Zhang (2001) simplified the analytical model of Yu and Singh (1989), producing a methodology that relies on measurements of the advancing water front over crop fields and is therefore able to compute Manning's n without measurements of the water surface elevation. Straatsma (2009) employed a 3-dimensional float tracking apparatus along with Acoustic Doppler Current Profiler (ADCP) data to provide the field measurements that were then used to derive roughness values using the Chézy equation. This general method and its derivative innovations provide a counterpoint to the method presented herein.

Direct measurement of bottom friction coefficient in the field has been applied most notably by Arcement and Schneider (1989). In this study, the method of Petryk and Bosmajian (1975) was adapted with the vegetation density of the trees and the soil grain size distribution measured directly, along with estimations of Manning's n values to account for microtopography (Strelkoff et al., 2000), non-living obstacles (debris, stumps, boulders, etc.) and low lying vegetation. De Doncker et al. (2009) was able to compute Manning's n as a function of the amount of biomass (measured in grams per square meter) in a river channel. The contribution of the soil to the overall roughness has also been a topic of research, largely from an irrigation perspective. Limerinos (1970) developed a method which was employed by Arcement and Schneider (1989) based on percentiles of the soil grain size distribution, following Strickler (1923). Gomez (1993) used flow measurements and profile photography to compute the roughness of stable armored gravel beds without relying on characteristic grain size. Gomez et al. (2005) employed the chain method of Saleh (1993) to measure the roughness of the soil.

For parameterizing overland flow models in practice, researchers and engineers rely on published results of the above-referenced work coupled with engineering judgment. Barnes (1967) and Arcement and Schneider (1989) provide photos of river reaches and floodplains where Manning's n has been computed to provide the engineer with a reference image for comparison to his/her project area. There are also references that provide tables of value ranges for different types of channels and floodplains, most notably those found in textbooks such as Chow (1959), French (1985) and Chow et al. (1988). Jakubis (2000) provides a list of recommended values from the literature. However, almost unanimously, the authors caution the application of published values to actual field situations.

In the case of hurricane storm surge inundation models, the roughness of the terrain surface exerts drag forces not only on the inundating flood wave, but also the prevailing winds that drive overland flows. In numerical models of this type, the winds serve as a forcing mechanism that transfers momentum to the water column by a stress (drag) applied at the air–sea interface. Frequently, the wind velocities are derived from meteorological models that produce spatially and temporally dynamic wind fields that assume open-ocean conditions (i.e. no obstacles above the ground or water surfaces). Wind forcing to the inundation model is usually comprised of observed data assimilated to the domain; Cardone and Cox (2009) describe this process in detail. However, above-ground obstacles upwind of a particular point serve to reduce the effective wind velocity at that point. As a result, parameters describing the canopy closure coverage and horizontal wind velocity reduction have been developed and applied to capture this effect (Westerink et al., 2008). Efforts to measure these parameters in the field mirror those of bottom friction coefficient. Analogous to the first methodology presented previously, researchers place anemometers throughout a field site or wind tunnel and measure the spatial variability of the wind field, followed by the computation of the corresponding roughness length based on average vegetation density and/or height (Sullivan and Greeley, 1993). Direct measurement of these parameters has been carried out by Lettau (1969) and improved upon by (Macdonald et al., 1998). Lookup tables of these values intended to assist practicing engineers with parameter selection are presented by Wieringa (1993), Simiu and Scanlan (1996) and Tieleman (2003). For engineering practice in the United States, the primary source for these values is the Federal Emergency Management Agency Multi-Hazard Loss Estimation Methodology manual (FEMA, 2006) which draws heavily from the work referenced above.

An automated parameterization scheme is required in order to implement these parameters in hurricane storm surge inundation models due to their typically large geographic scope. The direct measurement of surface roughness parameters at this scale is prohibitively expensive, if not impossible (Vieux and Farajalla, 1994). Since it is not feasible to compute the surface roughness parameters based on field measurements over the entire domain, modelers currently rely on land use/land cover (LULC) maps derived from remotely sensed data. Each LULC class has associated surface roughness parameter values; these values are then interpolated onto the mesh nodes and are incorporated into the model computations (Bunya et al., 2010; Westerink et al., 2008). While the accuracy and resolution of the published LULC data are progressing (Homer et al., 2007), the in situ conditions often differ significantly. This is especially true when one considers the needs of individual user groups. Biologists and planners rely on these data to conduct research and enhance decision making within a spatial framework; in fact, the LULC was initially used for assessing land use changes, modeling nutrient and pesticide loads in runoff, and assessing biodiversity and habitat preference (Vogelmann et al., 1998). However, for engineers or modelers that are concerned with the physical effect that terrain obstructions have on inundation flow or hurricane winds, the published data are sub-optimal and a more accurate description is necessary. While previous studies such as Werner et al. (2005) have demonstrated that reliance on values from the literature can be problematic, a direct comparison of surface roughness parameters based on LULC data and in situ measurements has not been carried out.

The research presented herein demonstrates this discrepancy by comparing the surface roughness characteristics computed based on field measurements and those assigned by the LULC method. This comparison is conducted for 24 sites in Florida and the results along with the associated statistics show that the in situ surface roughness parameters can differ substantially from those assigned by the LULC method.

2. Field measurement methods

Field measurements were conducted by a four person team at 24 sites on public land in Florida's Volusia, Lake and Franklin Counties from August 2010 to August 2011. More specifically, the field measurement sites were located in the Lake Monroe (LKMO), Seminole Forest (SEMF) and Hilochee (HILO) Wildlife Management Areas (WMA) and also the Apalachicola National Estuarine Research Reserve (ANER) as shown in Fig. 1. For clarity, these areas will be referred to as "locations" to distinguish them from the "sites" where the actual measurements took place. The 1992 and 2006 National Land Cover Dataset (NLCD) (Homer et al., 2007; Vogelmann et al., 2001) along with the 2006 Coastwatch Change Analysis Program (C-CAP; National Oceanic and Atmospheric Administration, 1995 – present) classifications for each site are shown in Table 1. The sites were selected in order to capture the common LULC types typical of Florida's Gulf coast, as shown in Table 2.

Each rectangular field measurement site measured 30 m by 15 m following Arcement and Schneider (1989) with the long edge running East–West as shown in Fig. 2. Site candidates were randomly plotted within the boundaries of the location and the field research team navigated to the site candidates using handheld Global Positioning Systems (GPSs). Site candidates were discarded if they were: located in areas closed by management staff; located in open water; inaccessible due to excessively dense understory vegetation; or deemed unsafe. Possible reasons for declaring a site unsafe include an excessive amount of stinging insects, poisonous plants or the presence of large broken tree limbs precariously suspended in the canopy. The team leader (corresponding author of this paper) also selected sites in order to achieve a range of surface roughness conditions typical in coastal areas in the southeastern United States at risk from hurricane storm surge including bare earth (e.g. parking lot, mowed grass field), areas of continuous or patchy tall grass and dense tree coverage. Once the site was established, it was demarcated using stakes and string aligned with magnetic compasses and measuring tapes. The coordinates for the site corners were obtained with handheld GPS in the Universal Transverse Mercator (UTM) projection and the World Geodetic System datum of 1984 (WGS84).

With the site boundary established, each member of the team independently estimated the bottom friction coefficients associated with each of the following: microtopography or relatively small undulations in the terrain within the site along with the presence of any depressions or conveyances; obstructions such as large rocks, stumps and debris; and low lying vegetation such as grasses, shrubs and seedlings. These estimations are taken according to the descriptions found in Table 3 and Figs. 6–20 of Arcement and Schneider (1989) and are necessary for computing Manning's *n*. The team leader instructed the participants on the estimation techniques and tested their aptitude on demonstration sites prior to obtaining actual study data.

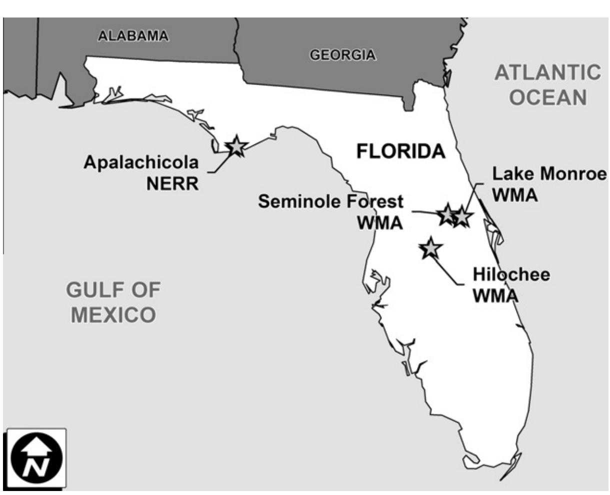

Fig. 1. Field measurement site locations.

Each team member independently estimated the surface canopy coverage at nine locations on site: the four site corners; the midpoint of each site boundary edge; and the exact center of the site. Estimations were obtained using a moosehorn measurement tool. This tool uses a mirror oriented to allow the researcher to see directly above him/her, assisted by vertical and horizontal leveling bubbles visible when looking into the device. Once the instrument is leveled, the researcher estimated the percentage of the field of view that is obscured by canopy.

The team then measured the dimensions of all above-ground obstructions present on the site. Obstructions were classified into three categories: trees, low lying vegetation and obstacles. Trees were defined by species and the presence of a defined trunk. Saplings and trees less than approximately 1 m in height were classified as low lying vegetation. Low lying vegetation also included shrubs, clumps of tall grasses and short palmetto clusters. Obstacles included stumps, dead trees, logs and debris. A photograph of each obstruction was taken with a GPS enabled camera (thereby also recording the geographic position). A reflector was attached to each subject obstruction being photographed in order to differentiate it from its surroundings.

For trees, the team obtained the following measurements: diameter of the trunk at breast height (D_{BH}); total height, taken with a laser hypsometer independently by two participants; height to the lowest significant branch (defined as the lowest branch that contributes to the canopy formation), taken with measuring tape or laser hypsometer independently by two participants (note that the two researchers taking this measurement also independently selected the lowest significant branch in addition to measuring its height); and width of the tree's canopy in both north–south and east–west directions. For trees with split trunks or clusters of like trees that share the same canopy, the diameters were measured and combined using a modified circle packing method. The cluster diameter was computed according to the following equation:

$$\text{for} \begin{cases} N < 3, & D_0 = \sum D_n \\ N = 3, & D_0 = \sum D_1, D_2 \\ N > 3, & D_0 = 2.91 D_{avg} + 0.107 \sum D_n \end{cases} \tag{1}$$

where N = number of trees in the cluster; D_0 = the minimum cluster diameter (m); D_n = individual D_{BH} of trees in the cluster; D_1, D_2 = the largest and second largest D_{BH} in the cluster, respectively; and D_{avg} = average D_{BH} in the cluster. For the case of $N > 3$, the work of Huang et al. (2002) was adapted. This work applies a heuristic algorithm to solve the problem of determining the minimum radius of a cluster of unequal circles. A testing data set consisting of a group of circles with unequal radii and their corresponding minimum cluster radius was presented. This data set was used here to develop the multiple regression function. This function describes the diameter of a cluster of unequal circles based on the average diameter and sum of the diameters of the trees in the cluster.

For low lying vegetation, the team obtained the following measurements: total height taken with measuring tape; total width of the vegetation in the north–south and east–west directions. In some instances, multiple plants in contact or in close proximity to one another were grouped and measured as one. Low lying vegetation was given a blaze orange backdrop for the photograph in order to distinguish it from its surroundings. The species of the vegetation was also recorded. The measurements for obstacles were identical to those of low lying vegetation, except that instead of species, a brief description of the obstacle was recorded.

Lastly, a topsoil sample of approximately 1.5–2 kg was taken from an open area as close as possible to the center of the site.

Table 1
Land use/land cover classifications of field measurement sites.

Site	1992 NLCD	2006 NLCD	2006 C-CAP
ANER-01	31 – Bare rock/sand	24 – Developed, high intensity (67%)	2 – High-intensity developed (66%)
		31 – Barren land (33%)	20 – Bare land (34%)
ANER-02	31 – Bare rock/sand	31 – Barren land	20 – Bare land
ANER-03	42 – Evergreen forest	52 – Shrub/scrub (58%)	8 – Grassland (53%)
		71 – Grassland/herbaceous (42%)	12 – Scrub/shrub (47%)
ANER-04	31 – Bare rock/sand	24 – Developed, high intensity	2 – High-intensity developed (89%)
			20 – Bare land (11%)
ANER-05	91 – Woody wetland	90 – Woody wetlands	13 – Palustrine forested wetland (1%)
			14 – Palustrine scrub/shrub wetland (99%)
ANER-06	31 – Bare rock/sand	31 – Barren land	20 – Bare land
ANER-07	91 – Woody wetland	52 – Shrub/scrub (74%)	12 – Scrub/shrub (79%)
		90 – Woody wetlands (26%)	20 – Bare land (21%)
ANER-08	33 – Transitional (24%)	31 – Barren land	12 – Scrub/shrub (26%)
	71 – Grassland (50%)		20 – Bare land (74%)
	42 – Evergreen forest (26%)		
ANER-09	31 – Bare rock/sand	31 – Barren land	20 – Bare land
ANER-10	42 – Evergreen forest	95 – Emergent herbaceous wetlands	12 – Scrub/shrub (8%)
			18 – Estuarine emergent wetland (92%)
HILO-01	71 – Grassland	90 – Woody wetlands	13 – Palustrine forested wetland (21%)
			14 – Palustrine scrub/shrub wetland (79%)
HILO-02	42 – Evergreen forest	90 – Woody wetlands	13 – Palustrine forested wetland
HILO-03	91 – Woody wetland	90 – Woody wetlands	13 – Palustrine forested wetland
LKMO-01	42 – Evergreen forest	90 – Woody wetlands	13 – Palustrine forested wetland
LKMO-02	71 – Grassland	21 – Developed, open space	5 – Developed open space (88%)
			14 – Palustrine scrub/shrub wetland (12%)
LKMO-03	71 – Grassland (85%)	21 – Developed, open space	13 – Palustrine forested wetland
	85 – Rec. grass (15%)		
LKMO-04	92 – Herbaceous wetland	90 – Woody wetlands (92%)	14 – Palustrine scrub/shrub wetland (97%)
		95 – Emergent herbaceous wetlands (8%)	15 – Palustrine emergent wetland (3%)
SEMF-01	92 – Herbaceous wetland (94%)	52 – Shrub/scrub	10 – Evergreen forest (20%)
	11 – Open water (6%)		12 – Scrub/shrub (80%)
SEMF-02	42 – Evergreen forest (68%)	52 – Shrub/scrub (70%)	10 – Evergreen forest (62%)
	51 – Shrub land (29%)	42 – Evergreen forest (30%)	12 – Scrub/shrub (38%)
	92 – Herbaceous wetland (3%)		
SEMF-03	91 – Woody wetland	52 – Shrub/scrub	12 – Scrub/shrub
SEMF-04	31 – Bare rock/sand	81 – Pasture hay (93%)	7 – Pasture/hay
		42 – Evergreen forest (7%)	
SEMF-05	91 – Woody wetland (88%)	52 – Shrub/scrub	12 – Scrub/shrub
	33 – Transitional (12%)		
SEMF-06	33 – Transitional (91%)	71 – Grassland/herbaceous (61%)	4 – Low-intensity developed (93%)
	23 – Commercial (9%)	52 – Shrub/scrub	7 – Pasture/hay (7%)
SEMF-07	42 – Evergreen forest (68%)	42 – Evergreen forest	10 – Evergreen forest
	91 – Woody wetland (32%)		

Table 2
Land use/land cover distribution within 20 km of Florida's Gulf coast shoreline.

2006 NLCD class	Percent of land area in Gulf coastal Florida (%)
52 – Shrub/scrub	23
82 – Cultivated crops	16
71 – Grassland herbaceous	15
42 – Evergreen forest	13
41 – Decidous forest	12
81 – Pasture hay	7
90 – Woody wetlands	4
21 – Developed, open space	3
43 – Mixed forest	2
22 – Developed, low intensity	2
95 – Emergent herbaceous wetlands	1
31 – Barren land	1
23 – Developed medium intensity	1
24 – Developed, high intensity	0

[a] LULC class open water was removed prior to computing percentages.

The research team first removed any extraneous materials (e.g., leaf litter) from the sample site and then proceeded to remove the soil sample to a depth of approximately 10 cm. The sample was subjected to a sieve analysis in order to determine the grain size distribution of the topsoil according to ASTM Standard C136-06. The sieve stack consisted of the following mesh sizes: #10 (2.000 mm); #16 (1.180 mm); #20 (0.850 mm); #40 (0.425 mm); #60 (0.250 mm); #100 (0.150 mm); and #200 (0.075 mm). This set is suitable for the medium sands typical of Florida topsoil.

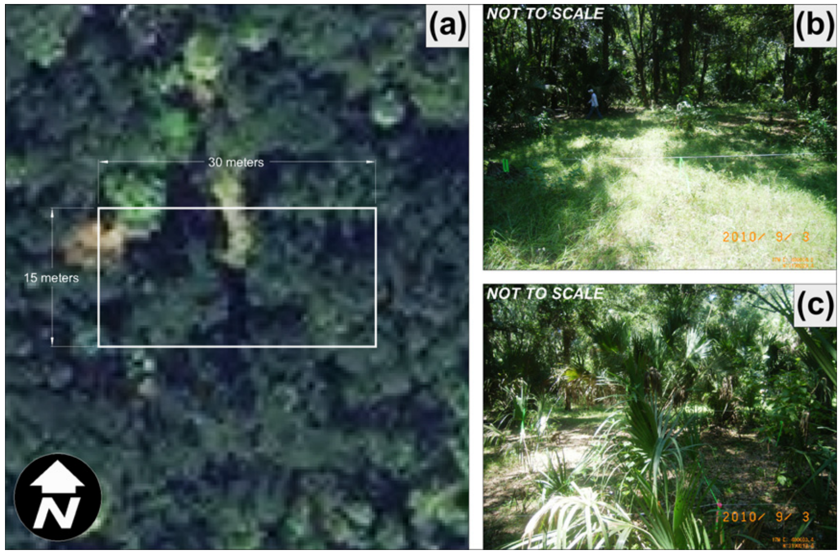

Fig. 2. Site layout example: (a) Aerial view of site boundary; (b) ground level view of site, looking south; (b) ground level view of site, looking west.

Table 3
Comparison of Manning's *n* values computed from field measurements and those assigned by 1992 NLCD.

Site	Manning's *n*			Range from literature based on in situ condition
	NLCD	Field	Error	
ANER-01	0.040	0.035	0.005	0.020–0.050
ANER-02	0.040	0.024	0.016	0.035–0.070
ANER-03	0.180	0.029	0.151	0.040–0.080
ANER-04	0.040	0.013	0.027	0.013
ANER-05	0.140	0.046	0.094	0.070–0.160
ANER-06	0.040	0.032	0.008	0.020–0.035
ANER-07	0.140	0.031	0.109	0.040–0.080
ANER-08	0.089	0.023	0.066	0.035–0.070
ANER-09	0.040	0.022	0.018	0.018–0.030
ANER-10	0.180	0.050	0.130	0.040–0.100
HILO-01	0.035	0.043	−0.008	0.030–0.050
HILO-02	0.180	0.030	0.150	0.035–0.060
HILO-03	0.140	0.035	0.105	0.040–0080
LKMO-01	0.180	0.031	0.149	0.050–0.080
LKMO-02	0.035	0.045	−0.010	0.035–0.055
LKMO-03	0.034	0.050	−0.016	0.070–0.160
LKMO-04	0.035	0.041	−0.006	0.050–0.110
SEMF-01	0.034	0.037	−0.003	0.022–0.035
SEMF-02	0.144	0.061	0.083	0.045–0.110
SEMF-03	0.140	0.052	0.088	0.035–0.070
SEMF-04	0.040	0.045	−0.005	0.035–0.065
SEMF-05	0.135	0.055	0.081	0.045–0.095
SEMF-06	0.095	0.017	0.079	0.025–0.055
SEMF-07	0.167	0.047	0.121	0.040–0.080
RMSE			0.083	

3. Calculations

The measurements taken in the field provided a data set that required careful processing, with the computation of each parameter requiring a unique approach to the utilization of the field measured data. The process for calculating each surface roughness parameter is presented in detail below.

3.1. Determining Manning's n

The determination of the bottom friction coefficient Manning's *n* proceeded according to methodology established by Arcement and Schneider (1989). While the general methodology was closely followed, some modifications were implemented. Please note that the term *R* appears in several places throughout the Manning's *n* computation process. This value represents the hydraulic radius, which for floodplains is equal to the flood depth. While it is widely known that Manning's *n* is sensitive to the depth of flow, for the purposes of this research, the flood depth is assumed to be 1 m. This value was chosen because it represents a reasonable base value to develop Manning's *n* coefficients that will in turn be varied with depth within numerical tidal and storm surge models. For example, the ADCIRC model employs a hybrid bottom friction formulation that computes an adjusted bottom friction coefficient based on Manning's *n* and flow depth at each time step (Luettich and Westerink, 2006).

The modifications to the Manning's equation proposed by Petryk and Bosmajian (1975) were used, given in the following form for SI units:

$$n = n_0\sqrt{1 + (Veg_d)\frac{C_*}{2g}R^{2/3}} \tag{2}$$

where n = Manning's n for the sample area at the specified flow depth; n_0 = base or boundary roughness Manning's n associated with all drag forces except those caused by trees; Veg_d = Vegetation density (m^2/m^3), or the fraction of the cross-sectional flow area occupied by tree trunks; C_* = Effective bulk drag coefficient of vegetation; R = hydraulic radius (m); g = acceleration due to gravity (m/s^2).

The effective bulk drag coefficient of vegetation, C_*, is computed based on Fig. 4 in Arcement and Schneider (1989).

The computation of the base Manning's n consists of summing the contributions from the topsoil (n_b), microtopography or surface irregularities (n_1), obstacles in the flood plain (n_3) and low lying vegetation (n_4):

$$n_o = (n_b + n_1 + n_2 + n_3 + n_4)m \tag{3}$$

Please note that m and n_2 are neglected as they are artifacts from the method's original application to channels. The n_2 term is neglected because it represents the contribution from the variance of the shape and size of the flow cross-section to the overall friction coefficient; this value is assumed to be zero because a floodplain is considered to be an infinitely wide, consistent cross-section. Also, m is a parameter that remains from this equation's original application to channels; it represents a correction factor accounting for the sinuosity or meandering of the channel. In the case of a floodplain, m = 1.0 because the length of the flow path and valley length are equal (Arcement and Schneider, 1989).

The value for the friction coefficient of the topsoil was calculated based on the following equation (Limerinos, 1970) modified for SI units (Marcus et al., 1992):

$$n_b = \frac{0.1129R^{1/6}}{1.16 + 2.0\log\left(\frac{R}{d_{84}}\right)} \tag{4}$$

where d_{84} = the 84th percentile diameter from the in situ soil sample (m). Aberle and Smart (2003) showed that grain size percentile method for computing bottom friction, as employed here, is ineffective when the flow depth is of the same order of magnitude as the grain size. This is the case on steep, rocky slopes such as mountain streams. However, in the case of coastal circulation and hurricane storm surge models, the soil types are typically fine to medium grained sands with flow depths multiple orders of magnitude greater than grain size. Therefore, this method is sufficient for this application. Also, sites or sections of sites that contained asphalt were given the Manning's n value of 0.013 (Chow, 1959).

The average estimates of n_1, n_3, and n_4 obtained by the participants on each site were also used in the calculation of n_0. Obvious outliers caused by recording errors were discarded from the averages; these were identified by computing the *z-score* of each estimation (Mendenhall and Sincich, 2007) according to the following formula:

$$z = \frac{y - \bar{y}}{s} \tag{5}$$

where y = participant estimated value; $\bar{y}$ = the mean estimated value (in this case the average estimate from the four participants); and s = standard deviation of estimates from the four participants. Estimates with *z-scores* greater than 2 were discarded.

Vegetation density was computed using the "Direct Technique" of Arcement and Schneider (1989):

$$Veg_d = \frac{R\sum D_{BH}}{Rwl} \tag{6}$$

where R = hydraulic radius (m); D_{BH} = diameter at breast height of tree trunk (m); w = width of site (m); l = length of site (m).

3.2. Determining surface canopy coverage

The surface canopy coverage for the site is computed by averaging the estimation taken by each participant at each location. The *z-score* criteria for identifying and discarding outliers presented in Section 3.1 were also used here. The coverage percentages for all nine measurement locations (C_p) are averaged to determine the canopy coverage fraction for the site (C_s).

3.3. Determining effective roughness length

The effective roughness length is an anisotropic parameter that reduces the horizontal velocity of the wind at a given point. The wind velocity reduction experienced at any given point will be different based on the wind direction due to differing upwind land cover characteristics. To provide a usable parameter to storm surge inundation modelers, the effective roughness lengths for 12 wind directions were computed based on the following formula (Lettau, 1969):

$$\vec{z_0} = 0.5\frac{H\vec{S}}{A} \tag{7}$$

where H = average height of all trees, low lying vegetation and obstacles (m); $\vec{S}$ = average frontal or silhouette area "seen" by the wind from each direction (m^2); A = total land area occupied by the roughness elements or the area of the field measurement site. The formulas for each term are presented below.

$$H = \frac{\sum_1^N H_n}{N} \tag{8}$$

$$S = \frac{\sum_1^{N_t} S_t + \sum_1^{N_l} S_l + \sum_1^{N_o} S_o}{N} \tag{9}$$

$$A = \frac{wl}{N} \tag{10}$$

where H_n = height of individual roughness element (m); N = total number of roughness elements; N_t = number of trees; N_l = number of low lying vegetation elements; and N_o = number of obstacles. Special consideration is given to the frontal or silhouette area. Similar to Jasinski and Crago (1999), the frontal profile for trees is assumed to be a half-ellipsoid on a post and is calculated as follows:

$$S_t = (H_{SB}D_{BH}) + F_{FA}\frac{\pi(H_T - H_{SB})(D_c/2)}{2} \tag{11}$$

where S_t = silhouette area of tree (m^2); H_{SB} = height to the lowest significant branch (m); D_{BH} = diameter at breast height (m); F_{FA} = fraction of frontal area occupied by leaves and branches, as opposed to empty space; H_T = total height of tree (m); and D_c = diameter of canopy (direction dependent, m). The frontal areas of low lying vegetation and obstacles are computed in similar fashion:

$$S_l = F_{FA}\frac{\pi(H_l)(D_l/2)}{2} \tag{12}$$

$$S_o = F_{FA}\frac{\pi(H_o)(D_o/2)}{2} \tag{13}$$

where S_l = silhouette area of low lying vegetation element (m^2); H_l = height of low lying vegetation element (m); D_l = diameter of low lying vegetation element (m); S_o = silhouette area of obstacle

(m^2); H_o = height of obstacle (m); and D_o = diameter of obstacle (m). As shown, low lying vegetation elements and obstacles are approximated as half-ellipses. The value of F_{FA} is assumed to be 0.5 for all types of vegetation and obstacles (FEMA, 2006).

In order to account for the directional dependency of the frontal area, the team measured diameters in the north–south and east–west directions for each roughness element in the field. These diameters form the basis of an elliptical interpolation scheme that computes the frontal area facing each of the 12 directions of the effective roughness parameter. An example is shown in Fig. 3. The interpolated, intermediate diameters are calculated as follows, based on the inherent properties of an ellipse (Clynch and Garfield, 2006):

$$D_c = 2\sqrt{\frac{a^2}{1 + \left(\frac{a^2}{b^2} - 1\right)\sin^2\phi}} \tag{14}$$

where D_c = diameter of tree canopy (m); a = semi-major axial radius of the tree canopy (m); b = semi-minor axial radius of the tree canopy (m); and ϕ = angle measured from the east–west line (radians).

3.4. Determining parameters assigned by NLCD

A recent storm surge inundation study by Bunya et al. (2010) using the ADCIRC model (Luettich and Westerink, 2006; Luettich et al., 1992) is taken to be the current state of the art for applying surface roughness parameters based on LULC data. Although multiple LULC schemes are presented in that work, only the 1992 NLCD (Vogelmann et al., 2001) is used here. While 1992 data may seem outdated, it is the only data set presented in Bunya et al. (2010) that provides a ubiquitous set of classes and their respective surface roughness parameters. The others are state specific and would not provide a consistent parameterization for comparison. These data are delivered as a raster product with 30 m resolution and cover the entire conterminous United States. Manning's n values are taken from Table 5 in Bunya et al. (2010). Effective roughness length values are taken from Table 9 in Bunya et al. (2010). For the field measurement sites where multiple LULC classes are present within a site, an average value is used, weighted by area. No quantitative comparison of surface canopy coverage was performed as further research is yet to be done on the incorporation of fractional values into overland inundation models. In spite of this, the surface canopy coverage results are presented for completeness.

3.5. Comparison of parameters derived from the two methods

In order to compare the results from the two parameterization methods, the LULC method was assumed to be the predictor and the field measurement method was assumed to be the ground truth or observed value. Manning's n values were compared based on the Root Mean Square Error (RMSE) according to the following formula:

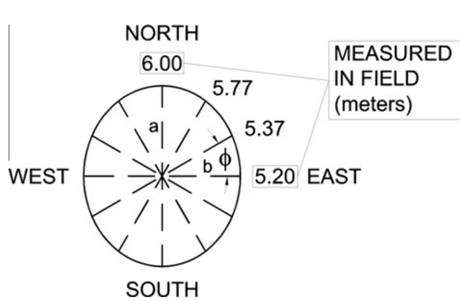

Fig. 3. Elliptical interpolation of tree canopy diameter.

$$\mathrm{RMSE} = \sqrt{N^{-1}\sum_{i=1}^{N}(P_i - O_i)^2} \tag{15}$$

where N = the number of comparisons (in this case, 24); P_i = the predicted (assigned by NLCD) value for the ith site; and O_i = the observed (computed based on field measurements) value. Manning's n values are also compared to a range of values based on in situ conditions at each site, guided by Chow (1959).

The effective roughness length used RMSE as the basis for comparison. Since the NLCD assigns a single value to a LULC class (rather than one for each direction), the average of the field measured values (in the 12 directions) was used for comparison purposes. Effective roughness length values are also compared to a range of values based on in situ conditions at each site and guided by Wieringa (1993) and Simiu and Scanlan (1996) as presented by FEMA (2006).

Lastly, a single sample *t-test* was applied to the absolute errors to determine the overall effectiveness of the NLCD method in selecting Manning's n and effective roughness length. This standard statistical test evaluated the null hypothesis that the mean of the absolute errors is zero (Mendenhall and Sincich, 2007). A two-tailed approach at a 95% confidence interval (α = 0.05) was used.

4. Results

The results for Manning's n, calculated versus assigned according to NLCD Land Cover class, are shown in Table 3. As stated on the summary line, the RMSE of the predicted values is 0.083. As the RMSE is similar in magnitude to the predicted and observed values of Manning's n, this represents a significant parameterization error for physically based models desiring to capture the physics of overland flow without automatic calibration. In fact, from the perspective of Manning's n, a RMSE of this magnitude can be considered approximately equivalent to erroneously parameterizing a High Density Residential area as Bare Rock/Sand. Compared to values published in the literature, the LULC method was within range on 25.0% of the sites, while the field measured values were within range on 50% of the sites.

The aerodynamic roughness values for surface canopy coverage and effective roughness length are presented in Tables 4 and 5, respectively. The maximum computed canopy coverage was 73% in a heavily forested area. The NLCD assigned effective roughness length values have a RMSE of 1.244 m. This is well within the magnitude of the predicted and observed values and in fact exceeds the average of the field measured values, making this an unacceptable level of error. From the perspective of effective roughness length, a RMSE of this magnitude can be considered approximately equivalent to twice the error that would result from erroneously parameterizing Shrub Land as Evergreen Forest. Compared to values published in the literature, the NLCD data was within range on 12.5% of the sites, while the field measured values were within range on 20.8% of the sites.

The absolute errors for the predicted and observed Manning's n and effective roughness lengths were compared using a single sample *t-test*. The results of this test, using a two-tailed approach and a 95% confidence interval (α = 0.05), are shown in Table 6 for Manning's n and effective roughness length, respectively. As shown in Table 6, the 95% confidence intervals for Manning's n and effective roughness length are 0.039–0.088 and 0.165–1.152 m, respectively. Therefore, we reject the null hypothesis that the mean absolute error is zero for both parameters. This indicates that the Manning's n and effective roughness length values predicted by LULC method were significantly different than those measured in the field.

Table 4
Surface canopy values computed from field measurements.

Site	Canopy coverage	Site	Canopy coverage	Site	Canopy coverage
ANER-01	0.00	ANER-09	0.00	LKMO-04	0.43
ANER-02	0.00	ANER-10	0.08	SEMF-01	0.15
ANER-03	0.04	HILO-01	0.00	SEMF-02	0.00
ANER-04	0.00	HILO-02	0.15	SEMF-03	0.17
ANER-05	0.13	HILO-03	0.00	SEMF-04	0.02
ANER-06	0.00	LKMO-01	0.73	SEMF-05	0.00
ANER-07	0.12	LKMO-02	0.25	SEMF-06	0.20
ANER-08	0.23	LKMO-03	0.63	SEMF-07	0.02

Table 5
Comparison of effective roughness values computed from field measurements and those assigned by 1992 NLCD.

Site	Effective roughness length (m)			Range from literature based on in situ conditions
	NLCD	Field	Error	
ANER-01	0.090	0.039	0.052	0.010–0.100
ANER-02	0.090	0.003	0.087	0.008–0.030
ANER-03	0.720	0.097	0.623	0.180–0.240
ANER-04	0.090	0.000	0.090	0.0002–0.0005
ANER-05	0.550	1.945	−1.395	0.900–1.000
ANER-06	0.090	0.004	0.087	0.0040–0.016
ANER-07	0.550	0.921	−0.371	0.650–0.800
ANER-08	0.252	0.100	0.152	0.170–0.240
ANER-09	0.090	0.011	0.080	0.004–0.015
ANER-10	0.720	1.182	−0.462	0.650–1.000
HILO-01	0.040	0.140	−0.100	0.02–0.06
HILO-02	0.720	0.689	0.031	0.650–0.800
HILO-03	0.550	0.195	0.355	0.350–0.450
LKMO-01	0.720	0.124	0.596	0.070–0.20
LKMO-02	0.040	0.187	−0.147	0.045–0.055
LKMO-03	0.041	4.658	−4.617	1.700–2.300
LKMO-04	0.110	3.399	−3.289	1.500–2.200
SEMF-01	0.103	0.962	−0.859	0.450–0.550
SEMF-02	0.530	0.039	0.491	0.250–0.400
SEMF-03	0.550	0.196	0.354	0.350–0.450
SEMF-04	0.090	0.610	−0.520	0.450–0.600
SEMF-05	0.506	0.061	0.445	0.200–0.450
SEMF-06	0.200	0.461	−0.261	0.500–1.000
SEMF-07	0.666	0.321	0.345	0.400–0.500
RMSE			1.244	

Table 6
Results of a two tailed *t*-test (95% confidence) on the absolute errors of the surface roughness values assigned by 1992 NLCD to those computed from field measurements.

Statistic	Absolute error	
	Manning's n	z_0
Mean	0.064	0.659
Standard deviation	0.054	1.078
Number of observations	24	24
Degrees of freedom	23	23
Standard error	0.011	0.220
t Statistic	5.766	2.993
p Value	0.000	0.006
Alpha	0.05	0.05
Alpha/2	0.025	0.025
Confidence interval	0.025	0.493
Lower confidence limit	0.039	0.165
Upper confidence limit	0.088	1.152

Table 7
Results of the comparison between surface roughness parameters assigned by 1992 NLCD to those computed from field measurements, broken down by LULC class.

1992 NLCD class[a]		Number of sites	Manning's n RMSE	z_0 RMSE (m)
31	Bare rock/sand	6	0.015	0.225
33	Transitional	2	0.072	0.214
42	Evergreen forest	6	0.133	0.469
71	Grassland	3	0.012	2.667
91	Woody wetland	5	0.096	0.712
92	Herbaceous wetland	2	0.005	2.403

[a] For sites where more than one LULC class is present, the dominant class is used.

Lastly, the errors in all parameters were not equal across the different LULC types encountered in the field. As shown in Table 7, the 1992 NLCD does a reasonable job at predicting Manning's n for Bare Rock/Sand, Grassland and Herbaceous Wetland areas but does an especially poor job predicting Manning's n for Evergreen Forest and Woody Wetland Areas. In terms of effective roughness length, the results are generally poor but contrary to the results of the Manning's n comparison, the 1992 NLCD data did a poor job predicting the values for Grassland and Herbaceous Wetland areas.

5. Discussion

The selection of techniques for direct measurement of roughness, especially for bottom friction, required a delicate balance of considerations including budget, available equipment, applicability, and scale. Kouwen and Fathi-Moghadam (2000) present an excellent work detailing the measurement of drag measurements on four species of conifer trees. Järvelä (2002, 2005) conducted flume experiments where both and non-submerged vegetation density were important factors in computing roughness, primary as a function of velocity. Baptist et al. (2007) induced equations describing the flow resistance due to vegetation that were refined using genetic programming and tested on both synthetic and actual laboratory testing data. Huthoff et al. (2007) developed an analytical solution to the problem of flow through submerged vegetation. This method reduces the vegetation density to a field of identical rigid cylinders in order to apply a standard drag force term. All of these methods increased the understanding of the flow processes at work when fluid flows through vegetation; however, they are not necessarily applicable to large scale parameterizations of highly mixed vegetation in variable flow fields influenced by outside factors such as wind and pressure, yet. These methods are without a doubt a step in this direction but the authors selected the method of Arcement and Schneider (1989) because it was developed for field conditions, is widely used in the United States and it contributed significantly to the development of the bottom friction lookup tables based on LULC data, as presented in Bunya et al. (2010) and Dietrich et al. (2011).

There are systematic factors concerning the field measurements and the associated computations that must be noted. The field measurements themselves contain systematic errors and in the case of Manning's n, rely on human estimates of surface roughness conditions. Furthermore, the computations of Manning's n and effective roughness length are based on empirically derived equations.

The primary sources of uncertainty in the field measurements are the estimations of the Manning's n components and surface canopy. Using the guidance provided in Arcement and Schneider (1989), in particular Table 3 of that report, the participants were all working from the same framework to estimate n_1, n_3 and n'_4. The participant estimates did differ but not to any significant degree. The average of the standard deviations for each parameter on each site are 0.0035, 0.0047 and 0.0032 for n_1, n_3 and n'_4, respectively. This was computed by determining the variance of each set of estimations (i.e. among the participants) on each site and computing the standard deviation of the set consisting of those values across all sites. The average standard deviation for the surface canopy estimates, computed in a similar manner was approximately 13%. This is reasonable considering the nature of the measurement and equipment used. On average, the estimations among the participants are reasonable and errors are managed by discarding outliers and averaging as explained in Section 3.1.

Some field measurements were carried out with equipment that has inherent systematic and random errors. Canopy diameters were measured using measuring tapes; on small vegetation this error was minimal as the participants could accurately determine the extents. However, for trees, the process involved determining the extent of the canopy visually and positioning beneath it. It is estimated that the canopy diameter measurements for tall trees could vary as much as plus or minus 0.5 m. An error bar of this magnitude does not significantly impact the computation of effective roughness length because for tall trees, their height tends to be the dominant factor and also they tend to have large diameters thereby minimizing the percentage of the measured diameter affected by the error.

The heights of the trees were measured using a laser hypsometer. Uncertainty in this measurement is influenced by the participant's judgment as to the location of the top of the tree. It is also influenced by the ability for the laser to accurately range the distance to the tree being measured; this is a problem in dense forests where the line of sight from the participant to the tree trunk is often obstructed. This source of uncertainty is minimized by taking two height measurements for each tree and averaging the result. These same sources of uncertainty are also present in the measurement of height to significant branch (H_{SB}). Throughout this research campaign, the tree height measurements and significant branch heights taken by the two participants differed by 0.64 and 0.35 m, respectively. These differences are minor and any error is minimized by averaging the two prior to the computations. There is also the added uncertainty due to the participant's selection of the significant branch, i.e. the lowest branch that contributes to the canopy. Due to the averaging of measurements from two participants, this error is also minimized.

There is also error in the comparison of results due to the use of handheld GPS technology to locate sites in the field. The handheld GPS used in this research has an accuracy of 2–5 m depending on the conditions (3 m was common). This may lead to spatially inaccurate classification of a sites LULC class and subsequently it's associated surface roughness parameters. Since the resolution of the 1992 NLCD data is 30 m, this error may be significant. However, this error is mitigated by using an area weighted average of the surface roughness parameters within a site.

The equations used to convert the field measurements into surface roughness parameters are largely empirical in nature. This is especially true of Eqs. (2) and (4). However, these equations are established in the literature and the studies that have occurred in this field since they were published. In the absence of a true physical measure of friction, or more fundamental, of energy loss, these equations are acceptable. They do, however, contain some variables whose values must be assumed in order to perform the computations.

Most obviously, the value of hydraulic radius, R, was assumed to be one meter. Recall that for a flood plain, R is equal to the depth of flooding. This is a realistic value for the primary application of this research to hurricane storm surge modeling. However, hurricane storm surges can range from fractions of a meter (on the order of one foot) to several meters such as those experienced in Mississippi during Hurricane Katrina (Knabb et al., 2011). Even considering this sensitivity to the assumed parameter of flood depth, coastal hydrodynamic models such as ADCIRC (Luettich and Westerink, 2006; Luettich et al., 1992) convert the specified Manning's n to a minimum bottom friction coefficient that varies quadratically with depth. Therefore, assuming a flood depth of one meter is reasonable for the parameterization of hurricane storm surge models.

The basis of the selection of surface roughness parameters using the NLCD data is the identification of the sites LULC classification. The 1992 NLCD classes for the sites used in this research are shown in Table 1. It is worth noting that coastal inundation modelers apply distance or area weighted interpolation schemes that factor in not only the LULC class at the exact location of a computational point, but include those in the surrounding area in as well. This minimizes the adverse effects of small pockets of a particular LULC class surrounded by a different one (Atkinson et al., 2011). However, the inherent variability within each LULC class, along with misclassification errors, still presents a problem for physics-based modelers. The interpolation schemes employed in practice serve to smooth out, but not eliminate, the errors associated with the LULC method for assigning surface roughness parameters. Another source of uncertainty in the results presented herein is the time elapsed between the acquisition of the remotely sensed data used to classify the LULC of the 1992 NLCD and the field measurements taken to compute competing surface roughness parameters. While this is certainly true as shown in Table 1, at its root, the primary contention of this research is not that the 1992 NLCD data are inaccurate, but rather that it was not designed to describe the surface roughness of the terrain and therefore does a sub-optimal job at doing so. Since 1992 NLCD data are the basis for parameterizing contemporary hurricane storm surge models, they make a good candidate for comparison. Even as LULC classifications become more accurate, the problem of the inherent variability within the LULC classes remains and therefore the unique roughness of the terrain at any given point in the domain will by definition be homogenized due to the categorical nature of LULC classes.

Even with these sources of uncertainty, only in a few cases were the field measured roughness parameters drastically different from the range given in the literature. This is to be expected since the ranges given in the literature require a significant amount of judgment and experience to apply, whereas computing the roughness values based on field measurements is a fairly straight forward procedure. It is interesting to note that the roughness parameters associated with LULC classes, regardless of scheme, were all generated based on the values published in the literature. This demonstrates how much the in situ roughness associated with a particular LULC class can vary from the "typical" conditions used to assign the parameters.

Further analysis of the relationship of both the surface roughness parameters predicted by NLCD data and computed using field measurements to the published ranges yields some interesting insights into the possible root cause of the errors. In this context, four error types emerge: (1) If both methods produced a value within the published range, the error is likely due to variability within the land cover class (17% and 8% of the sites had an error of this type for Manning's n and effective roughness length, respectively); (2) If the field measured value was within and the NLCD value was outside of the published range, the error is likely due to misclassification of the site (33% and 13% of the sites had an error of this type for Manning's n and effective roughness length, respectively); (3) If the field measured value was outside of and the NLCD value was within the published range, the error is likely due to the improper specification of the parameter for this LULC type. (17% and 8% of the sites had an error of this type for Manning's n and effective roughness length, respectively); and (4) If the both the field measured value and the NLCD value were outside of the published range, the source of the error is more difficult to determine and is likely the result of a combination of the three previous error types. This error type was the most prevalent as it was present on 33% and 71% of the sites type for Manning's n and effective roughness length, respectively.

6. Conclusions

In order to investigate the accuracy of assigning surface roughness parameters based on NLCD land cover classes, parameters were computed based on field measurements taken at 24 sites in Florida. The computed parameters were Manning's n bottom friction coefficient, surface canopy coverage, and effective roughness length. These three surface roughness parameters play a significant role in the modeling of tidal and storm surge flow over land.

The results of the study indicate that while parameterizing surface roughness using NLCD land cover data may be the best available practice at present, it is deficient. In terms of engineering modeling (i.e. roughness) parameters, the inherent variability within land cover classes, misclassification errors, and errors in the establishment of appropriate parameters for each land cover type (or often a combination of these error types) renders this methodology sub-optimal. Perhaps engineers and modelers would be better served by parameterizing surface roughness based on the physical structure of the terrain and the obstructions lying on it. However, typical coastal model domain sizes prohibit field campaigns sufficient in scope to properly parameterize the entire region of interest.

Therefore, an alternative approach may be to mine remotely sensed data such as airborne LiDAR (especially since the application of LiDAR is already required for FEMA coastal inundation digital elevation models) to describe the terrain roughness and enhance the parameterization of surface roughness. The use of these widely available data will facilitate applying the methodology at a regional or geographical scale. Work on this topic has been initiated by Menenti and Ritchie (1994), Straatsma and Middelkoop (2007) and Straatsma (2008) who were all able to develop parameterization schemes without reliance on categorical data such as LULC. However, work remains to be done to fully develop a method for parameterizing surface roughness, both bottom friction and aerodynamic roughness that is applicable to large scale hydrodynamic modeling. With that capability, a comparison between identical coastal inundation models, one parameterized using LULC data and one parameterized based on the physical terrain roughness described using remotely sensed data could be performed. This comparison would determine whether or not model performance is improved by a more physically-based parameterization of surface roughness. The mining of LiDAR data may also provide a means to easily parameterize fractional surface canopy coverage over a model domain and lead to its implementation in coastal inundation models, further reducing the uncertainty in this important parameter.

Acknowledgements

The authors wish to thank Matt Bilskie, Peter Bacopoulos, Ammarin Daranpob, Daina Smar, Davina Passeri and Amanda Tritinger for assisting with the field measurements. We also wish to thank the Florida Fish and Wildlife Conservation Commission, the Florida Division of Forestry, and the Florida Department of Environmental Protection for facilitating the field work on the lands in their charge. We are also deeply grateful to James Angelo for his advice on the presentation of the statistical results. This study is funded in part under NASA Grant Number NNX09AT44G. The statements, findings, conclusions, and recommendations expressed herein are those of the authors and do not necessarily reflect the views of NASA.

References

Aberle, J., Smart, G.M., 2003. The influence of roughness structure on flow resistance on steep slopes. J. Hydraul. Res. 41 (3), 259–269.
Arcement, G.J., Schneider, V.R., 1989. Guide for Selecting Manning's Roughness Coefficients for Natural Channels and Flood Plains.
Aricó, C., Nasello, C., Tucciarelli, T., 2009. Using unsteady-state water level data to estimate channel roughness and discharge hydrograph. Adv. Water Resour. 32, 1223–1240.
Atkinson, J.H. et al., 2011. Deriving frictional parameters and performing historical validation for an ADCIRC storm surge model of the Florida gulf coast. Florida Watershed J. 4 (2), 22–27.
Bacopoulos, P., Funakoshi, Y., Hagen, S.C., Cox, A.T., Cardone, V.J., 2009. The role of meteorological forcing on the St. Johns River (Northeastern Florida). J. Hydrol. 369, 55–70.
Bakry, M.F., Gates, T.K., Khattab, A.F., 1992. Field-measured hydraulic resistance characteristics in vegetation-infested canals. J. Irrigat. Drain. Eng. 118 (2), 256–274.
Baptist, M.J. et al., 2007. On inducing equations for vegetation resistance. J. Hydraul. Res. 45 (4), 435–450.
Barnes, H.H., 1967. Roughness Characteristics of Natural Channels. Water Supply Paper 1849. US Geological Survey.
Bunya, S. et al., 2010. A high-resolution coupled riverine flow, tide, wind, wind wave and storm surge model for southern Louisiana and Mississippi. Part I: model development and validation. Mon. Weather Rev. 138, 345–377.
Burguete, J., Garcìa-Navarro, P., Murillo, J., Garcìa-Palacìn, I., 2007. Analysis of the friction term in the one-dimensional shallow-water model. J. Hydraul. Eng. 133 (9), 1048–1063.
Cardone, V.J., Cox, A.T., 2009. Tropical cyclone wind field forcing for surge models: critical issues and sensitivities. Nat. Hazards 51, 29–47.

Chow, V.T., 1959. Open-Channel Hydraulics. McGraw-Hill Book Co., New York.
Chow, V.T., Maidment, D.R., Mays, L.W., 1988. Applied Hydrology. McGraw-Hill, Inc.
Clynch, J.R., Garfield, N., 2006. Equations of an Ellipse, pp. 1–14.
Cobby, D.M., Mason, D.C., Horritt, M.S., Bates, P.D., 2003. Two-dimensional hydraulic flood modelling using a finite-element mesh decomposed according to vegetation and topographic features derived from airborne scanning laser altimetry. Hydrol. Process. 17, 1979–2000.
De Doncker, L. et al., 2009. Determination of the Manning roughness coefficient influenced by vegetation in the river Aa and Biebrza river. Environ. Fluid Mech. 9, 549–567.
Dietrich, J.C. et al., 2011. Hurricane Gustav (2008) waves and storm surge: hindcast, synoptic analysis and validation in southern Louisiana. Mon. Weather Rev. 139, 2488–2522.
FEMA, 2006. Multi-hazard Loss Estimation Methodology – Hurricane Model – HAZUS MH MR3, Washington, DC.
French, R.H., 1985. Open Channel Hydraulics. McGraw-Hill, New York.
Galland, J.-C., Goutal, N., Hervouet, J.M., 1991. TELEMAC: a new numerical model for solving shallow water equations. Adv. Water Resour. 14 (3), 138–148.
Gomez, B., 1993. Roughness of stable, armored gravel beds. Water Resour. Res. 29 (11), 3631–3642.
Gomez, J.A., Vanderlinden, K., Nearing, M.A., 2005. Spatial variability of surface roughness and hydraulic conductivity after disk tillage: implications for runoff variability. J. Hydrol. 311, 143–156.
Harun-ur-Rashid, M., 1990. Estimation of Manning's roughness coefficient for basin and border irrigation. Agric. Water Manag. 18, 29–33.
Hervouet, J.M., 2000. TELEMAC modelling system: an overview. Hydrol. Process. 14, 2209–2210.
Homer, C. et al., 2007. Completion of the 2001 national land cover database for the conterminous United States. Photogram. Eng. Rem. Sens. 73 (4), 337–341.
Huang, W.Q., Li, Y., Gerard, S., Li, C.M., Xu, R.C., 2002. A 'Learning From Human' heuristic for solving unequal circle packing problem. In: Hao, J.K., Liu, B.D. (Eds.), First International Workshop on Heuristics. Tsinghua University, Beijing, China, pp. 39–45.
Huthoff, F., Augustijn, D.C.M., Hulscher, S.J.M.H., 2007. Analytical solution of the depth-averaged flow velocity in case of submerged rigid cylindrical vegetation. Water Resour. Res. 43, W06413.
Jakubis, M., 2000. A contribution to determination of the roughness coefficient of drainage and irrigation channels with clopes reinforced and grassing. J. Int. Commiss. Irrigat. Drain. 49 (3), 41–54.
Järvelä, J., 2002. Flow resistance of flexible and stiff vegetation: a flume study with natural plants. J. Hydrol. 269 (1–2), 44–54.
Järvelä, J., 2005. Effect of submerged flexible vegetation on flow structure and resistance. J. Hydrol. 307, 233–241.
Jasinski, M.F., Crago, R.D., 1999. Estimation of vegetation aerodynamic roughness of natural regions using frontal area density determined from satellite imagery. Agric. For. Meteorol. 94, 65–77.
Knabb, R.D., Rhome, J.R., Brown, D.P., 2011. Tropical Cyclone Report, Hurricane Katrina, 23–30 August 2005. National Oceanographic and Atmospheric Administration.
Kouwen, N., Fathi-Moghadam, M., 2000. Friction factors for coniferous trees along rivers. J. Hydraul. Eng. 126 (10), 732–740.
Lettau, H., 1969. Note on aerodynamic roughness-parameter estimation on the basis of roughness-element description. J. Appl. Meteorol. 8, 828–832.
Li, Z., Zhang, J., 2001. Calculation of field Manning's roughness coefficient. Agric. Water Manag. 49, 153–161.
Limerinos, J.T., 1970. Determination of the Manning coefficient from measured bed roughness in natural channels.
Luettich, R.A., Westerink, J.J., 2006. ADCIRC: A Parallel Advanced Circulation Model for Oceanic, Coastal and Estuarine Waters, adcirc.org.
Luettich, R.A., Westerink, J.J., Scheffner, N.W., 1992. ADCIRC: An Advanced Three-Dimensional Circulation Model for Shelves, Coasts, and Estuaries, Report 1: Theory and Methodology of ADCIRC-2DDI and ADCIRC-3DL. Vicksburg, Mississippi.
Macdonald, R.W., Griffiths, R.F., Hall, D.J., 1998. An improved method for the estimation of surface roughness of obstacle arrays. Atmos. Environ. 32 (11), 1857–1864.
Mailapalli, D.R., Raghuwanshi, N.S., Singh, R., Schmitz, G.H., Lennartz, F., 2008. Spatial and temporal variation of Manning's roughness coefficient in furrow irrigation. J. Irrigat. Drain. Eng. 134 (2), 185–192.
Marcus, W.A., Roberts, K., Harvey, L., Tackman, G., 1992. An evaluation of methods for estimating Manning's n in small mountain streams. Mountain Res. Develop. 12 (3), 227–239.
Mason, D.C., Cobby, D.M., Horritt, M.S., Bates, P.D., 2003. Floodplain friction parameterization in two-dimensional river flood models using vegetation heights derived from airborne scanning laser altimetry. Hydrol. Process. 17, 1711–1732.
Mendenhall, W., Sincich, T., 2007. Statistics for Engineering and the Sciences. Prentice Hall, Inc., Upper Saddle River, NJ, 1060pp.
Menenti, M., Ritchie, J.C., 1994. Estimation of effective aerodynamic roughness of Walnut Gulch watershed with laser altimeter measurements. Water Resour. Res. 30, 1329–1337.
Morvan, H., Knight, D., Wright, N., Tang, X., Crossley, A., 2008. The concept of roughness in fluvial hydraulics and its formulation in 1D, 2D and 3D numerical simulation models. J. Hydraul. Res. 46 (2), 191–208.
Myers, W.R.C., Knight, D.W., Lyness, J.F., Cassells, J.B., Brown, F., 1999. Resistance coefficients for inbank and overbank flows. Proc. Inst. Civ. Eng., Water, Maritime Energy 136 (2), 105–115.
National Oceanic and Atmospheric Administration, C.S.C., 1995 – present. The Coastal Change Analysis Program (C-CAP) Regional Land Cover. NOAA Coastal Services Center, Charleston, SC.
Petryk, S., Bosmajian III, G., 1975. Analysis of flow through vegetation. J. Hydraul. Div. 101(HY7), 871–884.
Saleh, A., 1993. Soil roughness measurement: chain method. J. Soil Water Conserv. 48 (6), 527–529.
Sepaskhah, A.R., Bondar, H., 2002. Estimation of Manning roughness coefficient for bare and vegetated furrow irrigation. Biosyst. Eng. 82 (3), 351–357.
Simiu, E., Scanlan, R.H., 1996. Wind Effects on Structures: Fundamentals and Applications to Design. John Wiley, New York.
Stephan, U., Gutknecht, D., 2002. Hydraulic resistance of submerged flexible vegetation. J. Hydrol. 269, 27–43.
Straatsma, M., 2009. 3D float tracking: in situ floodplain roughness estimation. Hydrol. Process. 23, 201–212.
Straatsma, M., Middelkoop, H., 2007. Extracting structural characteristics of herbaceous floodplain vegetation under leaf-off conditions using airborne laser scanner data. Int. J. Remote Sens. 28 (11), 2447–2467.
Straatsma, M.W., 2008. Quantitative mapping of hydrodynamic vegetation density of floodplain forests under leaf-off conditions using airborne laser scanning. Photogram. Eng. Rem. Sens. 74 (8), 987–998.
Strelkoff, T.S., Clemmens, A.J., Bautista, E., 2000. Field-parameter estimation for surface irrigation management and design. In: Flug, M., Frever, D. (Eds.), Watershed Management 2000 Science and Engineering Technology for the New Millennium. ASCE, Fort Collins, CO, pp. 10.
Strelkoff, T.S., Clemmens, A.J., Bautista, E., 2009. Estimation of soil and crop hydraulic properties. J. Irrigat. Drain. Eng. 135 (5), 537–555.
Strickler, A., 1923. Beiträge zur Frage der Geschwindigkeitsformel und der Rauhligkeitszahlen für Ströme, Kanäle und Geschlossene Leitungen. Mitt. des Eidgenössischen Amtes für Wasser-wirtschaft, p. 16.
Sullivan, R., Greeley, R., 1993. Comparison of aerodynamic roughness measured in a field experiment and in a wind tunnel simulation. J. Wind Eng. Ind. Aerodyn. 48, 25–50.
Tieleman, H.W., 2003. Roughness estimation for wind-load simulation experiments. J. Wind Eng. Ind. Aerodyn. 91, 1163–1173.
Vieux, B.E., Farajalla, N.S., 1994. Capturing the essential spatial variability in distributed hydrological modelling: hydraulic roughness. Hydrol. Process. 8, 221–236.
Vogelmann, J.E. et al., 2001. Completion of the 1990s National Land Cover Data Set for the conterminous United States from Landsat thematic mapper data and ancillary data sources. Photogram. Eng. Rem. Sens. 67, 650–652.
Vogelmann, J.E., Sohl, T.L., Campbell, P.V., Shaw, D.M., 1998. Regional land cover characterization using LANDSAT thematic mapper data and ancillary data sources. Environ. Monit. Assess. 51, 415–428.
Werner, M.G.F., Hunter, N.M., Bates, P.D., 2005. Identifiability of distributed floodplain roughness values in flood extent estimation. J. Hydrol. 314, 139–157.
Westerink, J.J. et al., 2008. A basin- to channel-scale unstructured grid hurricane storm surge model applied to southern Louisiana. Mon. Weather Rev. 136, 833–864.
Wieringa, J., 1993. Representative roughness parameters for homogeneous terrain. Boundary Layer Meteorol. 63, 323–363.
Xu, J.P., Wright, L.D., 1995. Tests of bed roughness models using field data from the Middle Atlantic Bight. Cont. Shelf Res. 15 (11/12), 1409–1434.
Yu, F.X., Singh, V.P., 1989. Analytical model for border irrigation. J. Irrigat. Drain. 115 (6), 982–998.